

Electronic conductivity and structural distortion at the interface between insulators SrTiO₃ and LaAlO₃

J.-L. Maurice^{*1}, C. Carretero¹, M.-J. Casanove², K. Bouzehouane¹, S. Guyard¹, É. Laroquet³, and J.-P. Contour¹

¹ Unité Mixte de Physique CNRS / Thales, associée à l'Université Paris Sud, Route départementale 128, 91767 Palaiseau cedex, France

² CEMES CNRS, 29 rue Jeanne Marvig, BP 94347, 31055 Toulouse cedex 4, France

³ IMPMC, Université P. & M. Curie, Campus Boucicaut, 75015 Paris, France

Received zzz, revised zzz, accepted zzz

Published online zzz

PACS 68.37.Lp, 68.47.Gh, 72.20.-i, 73.20.-r, 73.40.-c, 73.61.Ng.

When insulator LaAlO₃ is grown by epitaxy onto a TiO₂-terminated {100} surface of insulator SrTiO₃, the resulting system has a metallic character. This phenomenon has been associated with an electrostatic frustration at the interface, as {100} surfaces of SrTiO₃ are neutral while those of LaAlO₃ are polar, but its microscopic mechanism is not quite understood. Here, we present a structural characterisation of this interface by spherical aberration-corrected transmission electron microscopy. We show that the unit cells at the interface are elongated along the growth direction, and interpret this distortion in terms of Jahn-Teller effect.

1 Introduction

Perovskite oxides are the object of an increased attention due to their versatile properties that could lead to novel applications in microelectronics [1] and spintronics [2].

The generic perovskite oxide unit cell is a simple cube of formula ABO₃ where A and B are respectively a large and a small cation. In <100> directions, perovskites are stacks of {200} planes of alternate compositions AO and BO₂: there are thus two possibilities of stacking sequence at a {100} interface, which may have dramatically different properties depending on the valency of the different cations in presence. At the interface between the insulators LaAlO₃ (LAO) and SrTiO₃ (STO) for instance, the -LaO-TiO₂- and -AlO₂-SrO- sequences should present opposite electronic properties [3], the former donating, and the latter accepting, electrons [4]. Ohtomo and Hwang indeed detected high-mobility electrons in samples made of thin films of LAO grown onto TiO₂-terminated STO substrates (-LaO-TiO₂- sequence) while they found samples of LAO grown on SrO-terminated STO (-AlO₂-SrO- sequence) insulating [4].

We have grown LAO onto TiO₂-terminated STO in conditions similar to those used by Ohtomo and Hwang [4]. The aim of this paper is to present our results on interface characterisation at the atomic level. Our images show that the last TiO₆ octahedra in contact with LAO are elongated. We interpret this distortion in terms of a Jahn-Teller effect that would signal a lower average valency of the titanium ions at the interface.

2 Experimental

* Corresponding author: e-mail: jean-luc.maurice@thalesgroup.com

We have prepared the -LaO-TiO₂- interface by growing LAO onto TiO₂-terminated (001) STO using pulsed laser deposition [5]. The epitaxy was performed at a temperature of about 750°C and an oxygen pressure of 10⁻⁴ Pa maintained during cooling; it was controlled *in situ* by reflection high-energy electron diffraction. The substrate was commercial TiO₂-terminated (001) SrTiO₃. The thickness of the LAO films was varied from 7 to 22 nm. We measured the electrical conductivity with a four-probe equipment using contacts taken at different depths after ion etching (Fig. 1).

We then observed the interface at the atomic level by high-resolution transmission electron microscopy (HRTEM) using the SACTEM-Toulouse, a Tecnai G² F20 S-Twin equipped with a C_s corrector and automatic fine-tuning of astigmatism. Apart from the important enhancement of the resolution in the images, the main achievement of the C_s-corrector is that it substantially reduces contrast delocalization. The images of interfaces are thus considerably improved and can be easily interpreted. We also used a Jeol JEM 2100 equipped with a scanning stage and a high angle annular dark field (HAADF) detector. The intensity in such images depends only weakly on imaging conditions – contrary to HRTEM – so we could use such images as additional proofs that the distortions measured were intrinsic and not due to the imaging process.

The samples were thinned mechanically using the tripod technique down to a few μm, and then ion milled (Ar, 2 keV, 6°). This process unfortunately damaged the foil surfaces, especially on LAO, which considerably limited the spatial resolution attainable. We prepared cross sections perpendicular to <100> and <110> zones. {110} images of STO potentially contain more information [6], but our {110} samples were less robust than our {100}, so that their HRTEM images were finally not as significant. In the following, we present an HRTEM image of a {100} sample and an HAADF image of a {110} cross section. We did not attempt to localise pure oxygen columns, which needs very specific sample preparation and imaging conditions [6].

We used a two-fold approach to measure the distortions at the interface. (1) In order to get a statistically relevant result, we used a Fourier analysis of the images (HRTEM and HAADF), in which the local value of the 002 spatial frequency was mapped across the (001) interface [7] (see Fig. 2). Due to the finite size of the mask in this technique, the definition of the maps obtained, and the measured distortions, were spread over two to three (001) planes (~ 1 nm). (2) So we also analyzed the 002 lattice spacing in real space to get a better idea of the amplitude and localization of the effect, with conversely a larger uncertainty. In all cases, experimental images were part of defocus series and the actual defocus and thickness were determined by comparing with simulations [8].

3 Results

X-ray diffraction in the Bragg-Brentano geometry indicated that the lattice parameter of LAO in the growth direction was 0.378 nm, which corresponds to a 0.3 % decrease compared to the bulk parameter. Electron diffraction showed that growth was pseudomorphic in all samples observed, LAO adopting STO's in-plane parameter. Cubic STO has a bulk lattice parameter $a_{STO} = 0.3905$ nm and the pseudo-cubic unit cell of rhombohedral LAO has a parameter $a_{LAO} = 0.3792$ nm, so that $(a_{LAO} - a_{STO})/a_{STO} = -2.9\%$.

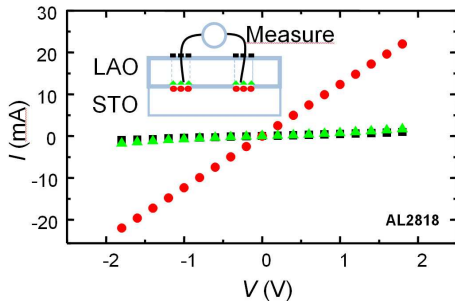


Fig. 1 (Colour online). Current-voltage curves recorded at 300 K on a LAO/STO sample, with contacts taken at different depths as shown in inset. Black squares correspond to contacts taken directly onto the LAO surface, green triangles, to contacts taken into the LAO film close to interface, after ion etching, red circles to contacts taken into STO just below interface. The four points were not aligned so that V/I ratios correspond to no meaningful resistance.

Applying isotropic elasticity theory, the in-plane and out-of-plane strains we have measured give the rather small Poisson ratio of 0.05 for LAO. A possibility is that the equilibrium lattice parameter of our LAO films was larger than that of standard material, which could indicate the presence of oxygen vacancies. No extended defects could be visualised, neither in HRTEM images nor in low-magnification, large-area pictures, which shows that no plastic relaxation occurred. A small disorientation between film and substrate was probably due to the rhombohedral distortion of LAO ($\sim 0.06^\circ$). In the case of the epitaxy of manganites on STO, which we have studied in detail, the rhombohedral distortion ($\sim 0.25^\circ$) is indeed recovered with no apparent defects within the first few nm above the interface [9].

Figure 1 shows current-voltage $I(V)$ curves recorded at an interface between a 20-nm thick LAO film and STO: depending on the depth at which the contact is taken, the system appears insulating (metallization separated from the interface by some LAO thickness), or conducting (metallization touching the interface). This conductivity was observed in all the samples analysed and it decreased with temperature.

Figure 2 summarises the analytical process we applied to HRTEM micrographs and indicates the magnitude and localisation of the distortion at the interface. The variations of amplitude of the 002 frequency (red dashed curve in Fig. 2c) show unambiguously that the perovskite unit cell is dilated at the interface. In the HRTEM image in Fig. 2a, where essentially AlO atomic columns are visible in LAO, the analysis of the intensity profile in real space (solid curve in Fig. 2c) indicates that the dilatation is localized on the interface unit cells. Its relative amplitude is +4.9 % while the standard deviation in the measurement of the spacing of all STO (001) planes in the image is $\pm 1.5\%$.

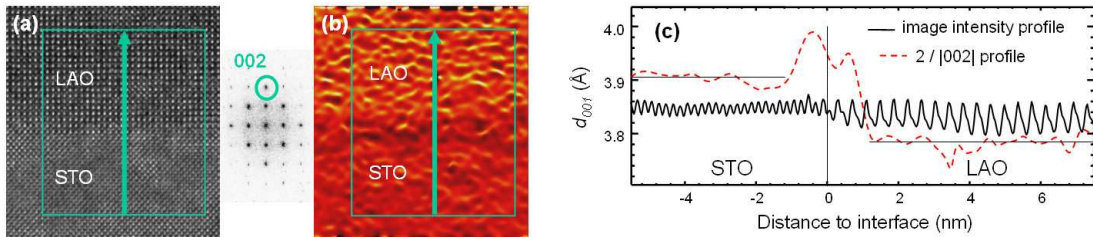


Fig. 2 (Colour online). The interface in $\{100\}$ cross section. (a) HRTEM image recorded at 200 kV, $C_s = 10 \mu\text{m}$, thickness 16 nm, defocus -18 nm. (b) Map of the modulus of the 002 spatial frequency. Scale is given by the arrows along which the intensity profiles were recorded. (c) Intensity profiles of (a) and (b), averaged parallel to interface as indicated by the green rectangles in (a) and (b). Twice the inverse of the $|002|$ value ($= d_{001}$) has been plotted instead of the direct intensity of (b), in order to better evidence the unit cell dilatation. The horizontal lines give the average values of the parameter in STO (0.3905 nm) and LAO (0.3784 nm); the vertical scale refers only to the $2/|002|$ profile, the scale of the image intensity is arbitrary.

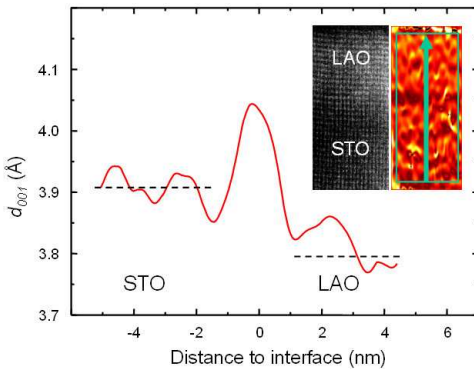


Fig. 3 (Colour online). (001) spacing profile deduced from a STEM-HAADF image of a $\{110\}$ cross section and its Fourier 002 map (insets). Dilatation of interface cells is clearly visible. The horizontal lines give the STO (0.3905 nm), and LAO (0.3784 nm) parameters.

In fact the dilatation was present in all images and in all the samples observed, but it was often difficult to localize due to noise. In another image taken in conditions where all cationic columns were visible in both materials, the dilatation was localized in between the SrO and LaO planes at the interface, i.e. on

the TiO₆ interfacial octahedra, and amounted to +9 % in the growth direction. However in that more noisy image, the standard deviation in (001) spacing was +/-5%. Although their uncertainty is large, these real-space measurements tend to show that TiO₆ octahedra are elongated by at least 4% at the interface. The Fourier analyses show the statistical relevance of the phenomenon. Finally, the measurement of this dilatation in HAADF images (Fig. 3) confirms its intrinsic nature.

4 Discussion and conclusion

Electrostatic equilibrium at the (001) interface between LAO and TiO₂-terminated STO requires the presence of one half extra electron per unit cell area [4]. Alternatively, it is equivalently obtained if one half of the Ti ions at the interface have valency 3+: $\text{La}^{3+}\text{Ti}^{3+}\text{O}^{2-}_3 \leftrightarrow \text{La}^{3+}\text{Ti}^{4+}\text{O}^{2-}_3 + \text{e}^-$. This flexibility of the system has however been invoked in discussing the relaxation of epitaxial stress [3]. In a simple ionic sketch, the 3d electron energy levels of Ti⁴⁺ are empty, while those of Ti³⁺ contain one electron. Solid state chemistry indicates that introducing a single electron in the 3d band of a 3d transition metal in octahedral symmetry will lead, in order to minimize the energy, to a distortion of the octahedron [10,11] by Jahn-Teller effect [12] (Fig. 4). The simplest explanation of the elongation observed here is that it is correlated by the Jahn-Teller effect with the presence of Ti³⁺ cations at the interface, which would be ‘unionised’ donors. EELS experiments are in progress to assess this hypothesis.

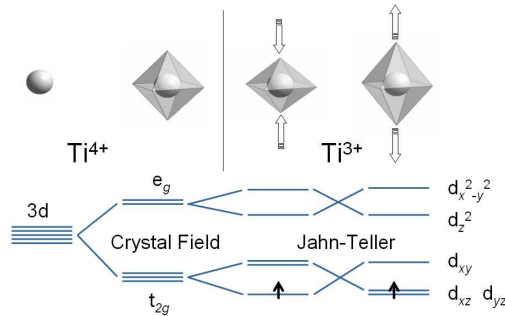


Fig. 4 Sketch of the correlations between site symmetry and electronic structure for Ti in an octahedral crystal field. Adding one electron to the 3d band should distort the octahedron by Jahn-Teller effect (energy shifts are arbitrary).

Acknowledgements We would like to thank M. Hÿtch (CNRS, Toulouse) for providing his image processing software of HRTEM spatial frequencies.

References

- [1] See e.g. K. Ueno, I. H. Inoue, T. Yamada, H. Akoh, Y. Tokura, and H. Takagi, Appl. Phys. Lett. **84**, 3726 (2004), and the references therein.
- [2] See e.g. H. Yamada, Y. Ogawa, Y. Ishii, H. Sato, M. Kawasaki, H. Akoh, Y. Tokura, Science **305**, 646 (2004) and the references therein.
- [3] D.-W. Kim, D.-H. Kim, B.-S. Kang, T. W. Noh, D. R. Lee, and K.-B. Lee, Appl. Phys. Lett. **74**, 2176 (1999).
- [4] A. Ohtomo and H. Y. Hwang, Nature (London) **427**, 423 (2004).
- [5] See more details in e.g. J.-L. Maurice, R. Lyonnet, J.-P. Contour, J. Magn. Magn. Mater. **211**, 91 (2000).
- [6] C. L. Jia, M. Lentzen, and K. Urban, Science **299**, 870 (2003).
- [7] M. J. Hÿtch, in: Stress and strain in epitaxy: theoretical concepts, measurements and applications, edited by M. Hanbÿcken and J.-P. Deville, (Elsevier, Amsterdam, 2001), p. 201.
- [8] P. A. Stadelmann, Ultramicroscopy **21**, 131 (1987).
- [9] J.-L. Maurice, F. Pailloux, A. Barthélÿmy, O. Durand, D. Imhoff, R. Lyonnet, A. Rocher, and J.-P. Contour, Philos. Mag. **83**, 3201 (2003).
- [10] B. Raveau, C. Michel, M. Hervieu and D. Groult, Crystal chemistry of high Tc superconductors, Springer series in materials science **15** (1991).
- [11] see also solid state chemistry text books, e.g. J.-F. Marucco, Chimie des solides (EDP Sciences, Les Ulis, 2004).
- [12] H. A. Jahn and E. Teller, Proc. R. Soc. London, Ser. A **161**, 220 (1937).